RSC Advances

PAPER

View Article Online
View Journal | View Issue

CrossMark click for updates

Cite this: *RSC Adv.*, 2016, **6**, 98109

Cucurbit[7]uril-threaded fluorene–thiophene-based conjugated polyrotaxanes†

M. Idris,[a] M. Bazzar,[ac] B. Guzelturk,[bc] H. V. Demir[bc] and D. Tuncel*[ac]

Received 29th August 2016
Accepted 10th October 2016

DOI: 10.1039/c6ra21622f

www.rsc.org/advances

Here we investigate the effect of cucurbit[7]uril (CB7) on the thermal and optical properties of fluorene–thiophene based conjugated polyelectrolytes. For this purpose, poly(9,9′-bis(6″-(*N*,*N*,*N*-trimethylammonium)-hexyl)fluorene-*alt*-*co*-thiophenelene) **P1** and poly(9,9′-bis(6″-(*N*,*N*,*N*-trimethylammonium)propyl)fluorene-*alt*-*co*-thiophenelene) **P2** and their CB7-based polyrotaxane counterparts, **P1CB7** and **P2CB7**, are synthesized by threading the part of the conjugated backbone of these polymers with CB7 during their synthesis. Threading efficiency in the **P1CB7** containing hexyl pendant of as high as 50% is achieved, but in the case of **P2**, with the propyl pendant, only around 15% is achieved. We observed significant changes in the optical properties of both **P1CB7** and **P2CB7** with respect to their polymers **P1** and **P2**. Fluorescent quantum yields of **P1** and **P2** which are 0.11 and 0.35 have increased to 0.46 and 0.55 for **P1CB7** (>4 fold) and **P2CB7**, respectively. Moreover, polyrotaxanes compared to their polymers exhibit longer fluorescence lifetimes in the solution and the solid state thanks to the suppressed overall nonradiative recombination *via* encapsulation of the conjugated polymer backbone. Thermal analysis also indicates that polyrotaxanes have higher thermal stabilities than their polymer counterparts. In order to demonstrate the applicability of the synthesized materials, we also fabricated proof-of-concept light emitting diodes from **P1** and its CB7-based polyrotaxane counterpart **P1CB7**. The CB7-integrating polymer showed lower turn-on voltages with high electroluminescence colour purity due to balanced charge injection in **P1CB7** as compared to the **P1** polymer.

Published on 11 October 2016. Downloaded by Bilkent University on 12/23/2018 11:24:34 AM.

Introduction

Conjugated polymers are very adaptable materials and as a result, can find many important applications including in light emitting diodes (LED), photovoltaic cells, solid state lighting, actuators and artificial muscles.[1–6] They are particularly appealing in the fabrication of LEDs for flexible and rollable display applications owing to their tunable optical properties (*e.g.* absorption, emission wavelengths and band gap) through judicious chemical modifications in their structures. Some of the important parameters regarding these polymers are fluorescent quantum yields, photo and thermal stabilities as well as the solubility. Their solubility properties can be tuned by attaching appropriate solubilizing groups to the backbone of the polymers by not harming the π-conjugation. Water solubility is also important to eliminate the use of harmful organic solvents and also for multilayer film formation to achieve different solubilities of the films (*e.g.*, using orthogonal solvents).[7–12] In order to render these polymers water-soluble, hydrophilic groups are used as pendant groups, however, due to the large aromatic hydrophobic backbone the water solubility could be still limited. The attachment of the ionic groups is another possibility but this can cause a quenching in their emission properties. Luminescence quenching is especially an important drawback when the polymer solutions are casted as a film for device fabrication. The morphology of polymers is considerably affected by both inter and intra-chain interactions; there are several approaches for controlling these. One of the reasons of the quenching is the π–π stacking between the polymer chains.[13] A number of different methods have been used to decrease the π–π stacking; for instance, attaching bulky pendant groups such as dendrons to polymer backbone, embedding polymers in silica nanoparticles or zeolites.[14–16]

Another promising approach is the encapsulation or insulation of conjugated polymer backbone by rotaxanation.[17,18] Rotaxanation is basically the threading of a polymer chain by a macrocyclic ring. The properties of polymers can be altered dramatically by the chemical nature of the macrocycle and the degree of threading. There are many examples on the use of cyclodextrins to insulate the conjugated polymer backbones,[19–21] however, examples are very scarce on the use of cucurbit[*n*]urils (CB[*n*]).[13,22–25] Cucurbiturils (CBs) are macrocycles with a rigid symmetrical structure that are composed of *n*

[a]*Department of Chemistry, Bilkent University, 06800 Ankara, Turkey. E-mail: dtuncel@fen.bilkent.edu.tr*

[b]*Departments of Electrical and Electronics Engineering and Physics, Bilkent University, 06800 Ankara, Turkey*

[c]*UNAM–National Nanotechnology Research Center, Institute of Materials Science and Nanotechnology, Bilkent University, Ankara 06800, Turkey*

† Electronic supplementary information (ESI) available. See DOI: 10.1039/c6ra21622f

Published on 11 October 2016. Downloaded by Bilkent University on 12/23/2018 11:24:34 AM.

glycoluril units (where $n = 5$, 6, 7, 8, 10, and 14) connected by methylene bridges and possess two identical hydrophilic portals with a hydrophobic cavity.[26–29] The diameter of the cavity varies depending on the number of glycoluril units. A variety of nanostructured materials including nanoparticles, nanocomposites, vesicles, rods have been prepared by taking advantage of the varying cavity size of the CB homologues, their ability to accommodate more than one guests in their cavities, their rigid symmetrical structures.[30–32] Moreover, they have been widely used to encapsulate and solubilize dyes.[33,34]

Herein, by taking advantage of the ability of CB7 to encapsulate the properly sized aromatic rings and water solubility, poly(9,9′-bis(6″-(*N*,*N*,*N*-trimethylammonium)hexyl)fluorene-*alt*-*co*-thiophenelene) **P1** and poly(9,9′-bis(6″-(*N*,*N*,*N*-trimethylammonium)propyl)fluorene-*alt*-*co*-thiophenelene) **P2** and their CB7-based polyrotaxane counterparts, **P1CB7** and **P2CB7** are synthesized by threading the part of conjugated backbone of these polymers with CB7 during their synthesis and their optical and thermal properties have been compared.

Results and discussion

Synthesis and structural characterization

All polymers and polyrotaxanes were synthesized according to reaction Scheme 1 in good yields. First, 2,7-dibromo-9,9-bis(6-bromohexyl)-9*H*-fluorene and 2,7-dibromo-9,9-bis(3-bromopropyl)-9*H*-fluorene were synthesized following the literature preparation,[35–37] and subsequently, they were converted into the monomers **M1** and **M2** respectively by treating with excess trimethylamine solution in tetrahydrofuran (THF) (Fig. S1–S10, ESI†). Polymers, **P1** and **P2** were synthesized by Pd-catalyzed Suzuki coupling of **M1** and **M2** with 2,5-thiophenediboronic ester. For the synthesis of polyrotaxanes, 2,5-thiophenediboronic ester and excess CB7 in aqueous solution were first stirred at 50 °C for 2 h to allow complexation of CB7 with 2,5-thiophenediboronic ester followed by the coupling reaction. The OH groups in 2,5-thiophenediboronic acid were protected using 1,3-propanediol from forming hydrogen bond with the carbonyl oxygens of CB7 so that inclusion of the thiophene into CB7 will not be hindered. Fig. S11† shows the spectra of 2,5-thiophenediboronic ester in the presence (3 folds excess of 2,5-thiophenediboronic ester) and in the absence of CB7. In order to remove excess, free CB7 and unreacted monomers and oligomers, the purification was carried out by ultrafiltration using a 5 kDa membrane against distilled water. The ultrafiltration was kept until the dialysates contain no free CB7 and other small molecules. Retentate solution was concentrated to a possible minimum volume and precipitated into excess acetone in order to remove the remaining catalyst residues. Dark green or dark yellowish precipitates were collected and dried under vacuum. We have also tried to use CB6 in the polyrotaxane synthesis but apparently due to low solubility of CB6 in water we could not obtain the desired polyrotaxanes.

Both polymers and the polyrotaxanes are soluble in water. **P1** and **P2** are also soluble in methanol however the solubility of the polyrotaxanes in methanol is very limited.

The structure of **P1**, **P2**, **P1CB7** and **P2CB7** were verified by ^{1}H NMR spectroscopies (Fig. 1 and 2). The broad peaks in the ^{1}H-NMR spectra of **P1** and **P1CB7** can be attributed to the chain entanglement due to the long hexyl side chain creating different environment of the protons in the structure. Comparing **P1** and **P1CB7** ^{1}H-NMR spectra, peaks at around 6.0–6.5 ppm in **P1CB7** spectrum can be assigned to the protons of thiophene which are encapsulated by CB7. The integration of these peaks reveals that approximately for every two repeating units in the polymer backbone, one thiophene is encapsulated by CB7 which corresponds to about a 50% threading efficiency.

^{1}H-NMR spectra of **P2** and **P2CB7** show less aggregation between the polymer chains. This can be explained by the shorter side chain of these polymers. Although the presence of CB7 is evident in the ^{1}H-NMR spectrum of **P2CB7**, no peak is observed around 6.0–6.5 ppm probably due to low contents of CB7. From the integration of signals of CB7 protons, the threading efficiency was calculated to be around 15% which corresponds to about every six repeating unit containing one CB7.

In order to further support the presence of CB7 due to the encapsulation of conjugated backbone rather than complexation with pendant, polymers **P1** and **P2** were separately mixed with CB7 at certain ratios and dissolved in dilute aqueous solution of HCl (around 0.01 M) and subsequently the solutions were subjected to the ultrafiltration as used in the purification of the aforementioned polymers and polyrotaxanes. ^{1}H-NMR spectrum of retentate recorded after the ultrafiltration showed the presence of only trace amount of CB7. This experiment indirectly proves that the presence of CB7 is due to the encapsulation of the part of the polymer main chain as aimed.

We have also recorded ^{1}H-NMR spectrum of the mixture of 2,7-dibromo-9,9-bis(6-bromohexyl)-9*H*-fluorene with CB7 in order to reveal whether CB is threaded onto hexyl pendant group. In the spectrum, no changes were observed in the chemical shifts of the methylene protons of the hexyl group. We have also reported this in our previous publication.[25] Although we can expect an ion–dipole interaction between ammonium ions and the carbonyl portals of the CB, there are a lot of potassium ions (coming from K_2CO_3 used as a base in the polymerization) which can compete with ammonium ions and complex with excess, free CB7.

Thus, the resulting complexes are removed during ultrafiltration/dialysis.

The reason of the higher threading efficiency in **P1CB7** compared to **P2CB7** can be explained by the side chain lengths of the fluorene monomers used. Monomer **M2** contains a short propyl pendant group and during Suzuki coupling, propyl group acts as a rigid moiety by preventing the CB7-thiophene diboronic ester being in close proximity due to steric effect. Whereas, monomer **M1** contains a flexible hexyl group that can flex itself during the coupling and not preventing CB7-thiophene diboronic ester to be in a closer contact.

These compounds were further characterized by FTIR spectroscopy (Fig. S14, ESI†). The peak at 1740 cm^{-1} for **P1CB7** and **P2CB7** suggests the presence of carbonyl group due to CB7

 This journal is © The Royal Society of Chemistry 2016

Published on 11 October 2016. Downloaded by Bilkent University on 12/23/2018 11:24:34 AM.

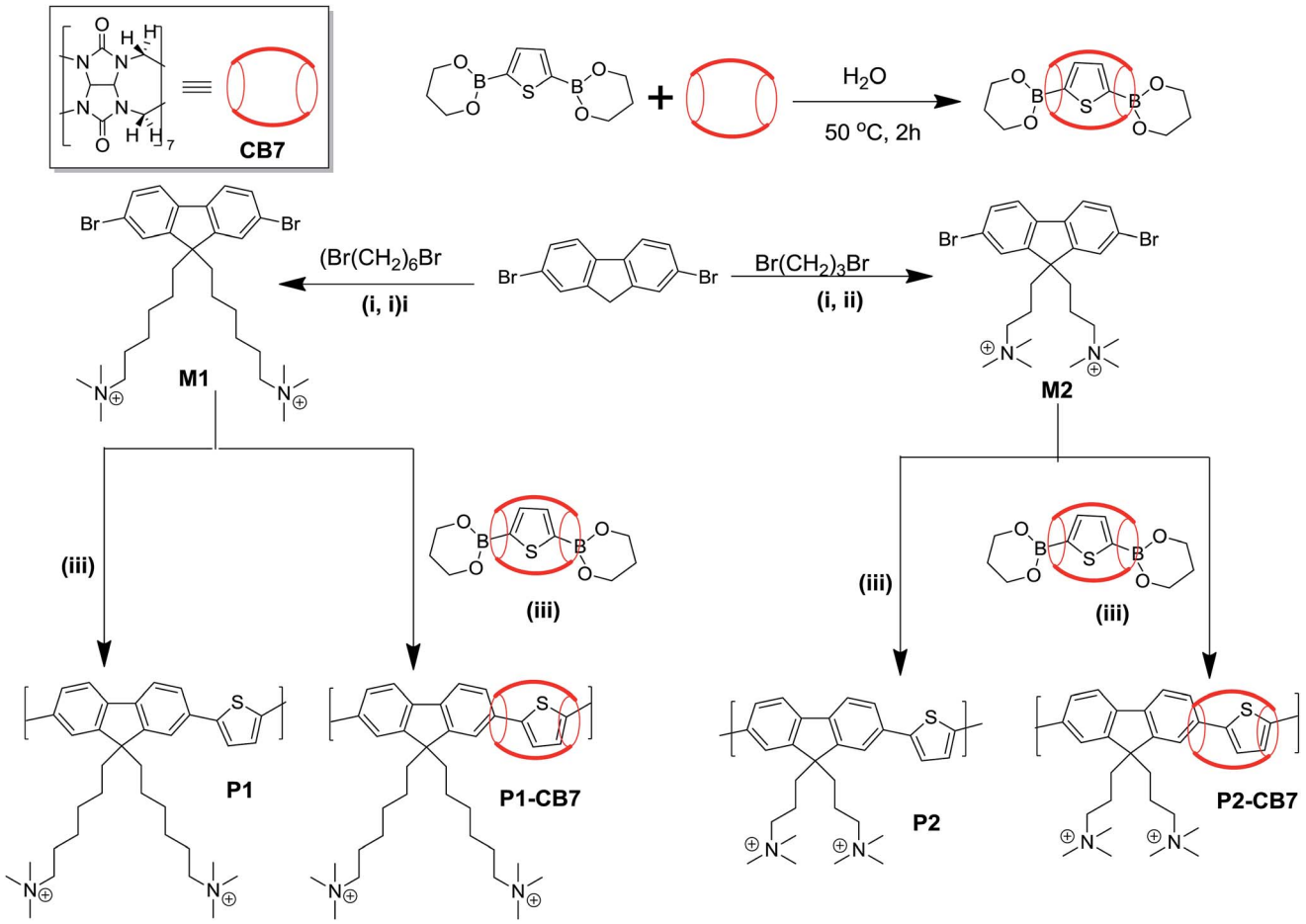

Scheme 1 Synthetic schemes for poly[9,9-bis{6(*N*,*N*,*N*-trimethylamino)hexyl}fluorene-*co*-2,5-thienylene (**P1**), poly[9,9-bis{3(*N*,*N*,*N*-trimethylamino)propyl}fluorene-*co*-2,5-thienylene (**P2**) and their CB7-based polyrotaxane counter parts **P1CB7** and **P2CB7**. Reaction conditions: (i) TBAB, 50% wt NaOH (aq), DMSO; (ii) Me_3N, THF, 25 °C, 24 h; (iii) $Pd(OAc)_2$, K_2CO_3, H_2O, 80 °C, 48 h.

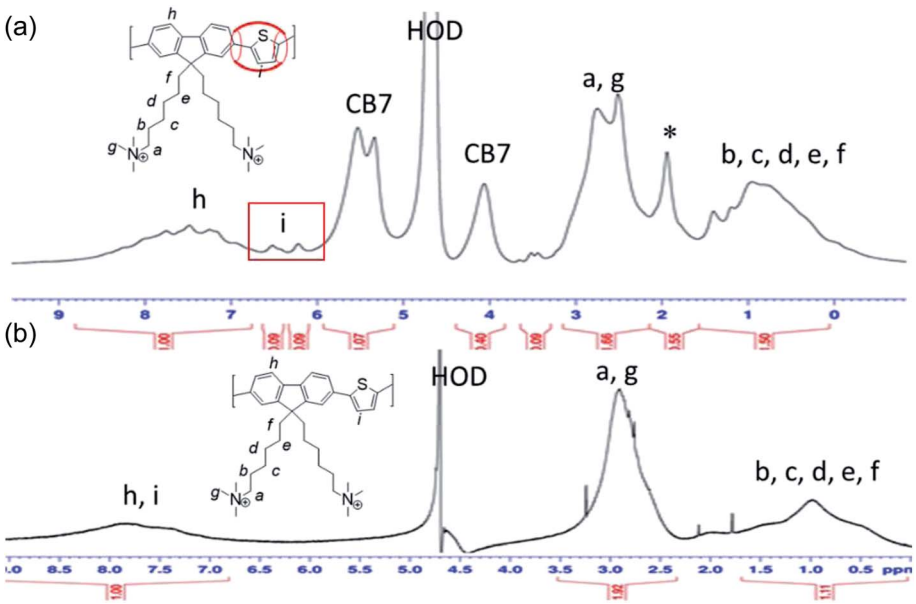

Fig. 1 ^{1}H-NMR (400 MHz, 298 K) spectra of (a) **P1CB7** in D_2O and (b) **P1** in D_2O. * denotes acetone residue.

Published on 11 October 2016. Downloaded by Bilkent University on 12/23/2018 11:24:34 AM.

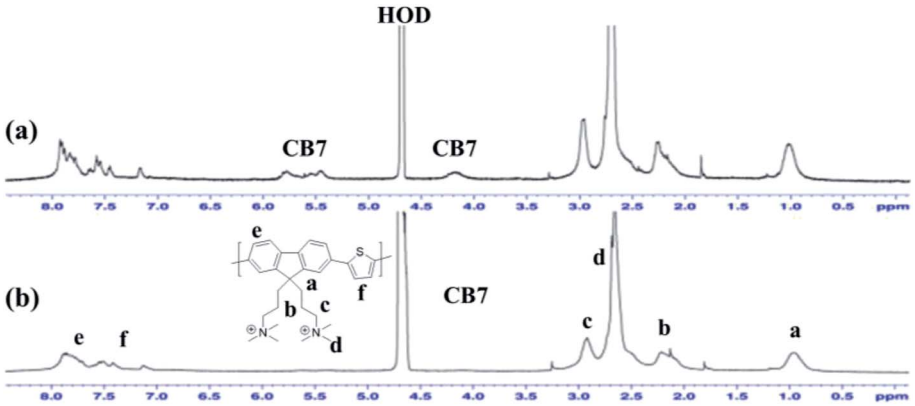

Fig. 2 ^{1}H-NMR (400 MHz, 298 K, D_2O) spectra of (a) **P2CB7** (b) **P2**.

which is absent in **P1** and **P2**. Although we have tried various conditions and solvents for molecular weight determination of all the polymers and polyrotaxanes using size exclusion chromatography (SEC), we were not able to obtain satisfactory results probably due to the irreversible adsorption of the polymer onto the column packing material due to the ionic charge on the polymers. However, ESI suggest a molecular weight up to 5000 Da with multiple charges of both polymers and polyrotaxanes. The estimate number of repeating units for polymers and polyrotaxanes would be around 7 and 2–3, respectively. However, ESI-MS is probably under estimating the real MW of the polymers and the polyrotaxanes owing to difficulty of the ionizing the large chains.

Thermal properties

The thermal stability of the polymers **P1**, **P2** and polyrotaxanes **P1CB7** and **P2CB7** were evaluated by thermal gravimetric analysis (TGA) under nitrogen atmosphere at a heating rate of 10 °C min^{-1}. Fig. 3 presents their TGA curves. Corresponding weight loss temperatures of 20% (T_{20}) and char yield-weight of polymers remained at 650 °C were all determined from original curves and listed in Table 1. Conversely, TGA profile of polymers shows that decomposition occurs in several steps, in which involves the decomposition of alkyl chains, ammonium groups and CB7. Polyrotaxanes **P1CB7** and **P2CB7** showed higher thermal stability than the corresponding polymers (**P1** and **P2**). The T_{20} value has increased from 205 to 240 °C for **P2CB7** and from 240 °C to 380 °C for **P1CB7**. Although both polyrotaxanes exhibit higher thermal stabilities than their polymer counterparts, polyrotaxane **P1CB7** with a higher threading efficiency than **P2CB7** starts to decompose even at

Table 1 Thermal properties of **P1**, **P2** and polyrotaxanes **P1CB7**, **P2CB7**

Polymers	T_{20}[a] (°C)	C. Y.[b] (%)
P1	240	47
P1CB7	380	40
P2	205	50
P2CB7	240	35

[a] T_{20}: temperature for 20% weight loss. [b] C. Y.: char yield-weight of polymer remained at 650 °C.

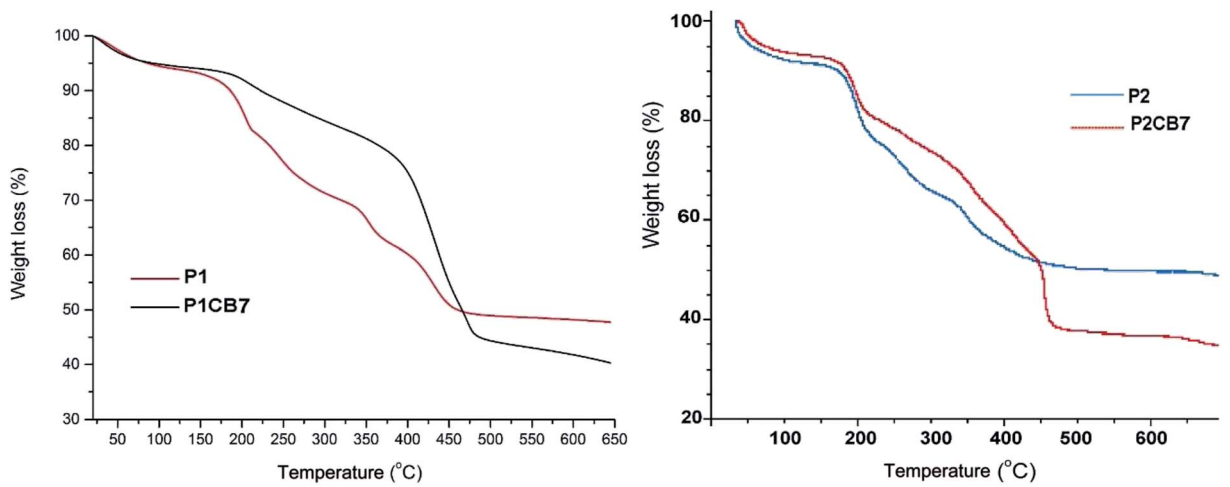

Fig. 3 TGA curves of polymers **P1**, **P2** and polyrotaxanes **P1CB7**, **P2CB7** under N_2 at 10 °C min^{-1}.

 This journal is © The Royal Society of Chemistry 2016

Published on 11 October 2016. Downloaded by Bilkent University on 12/23/2018 11:24:34 AM.

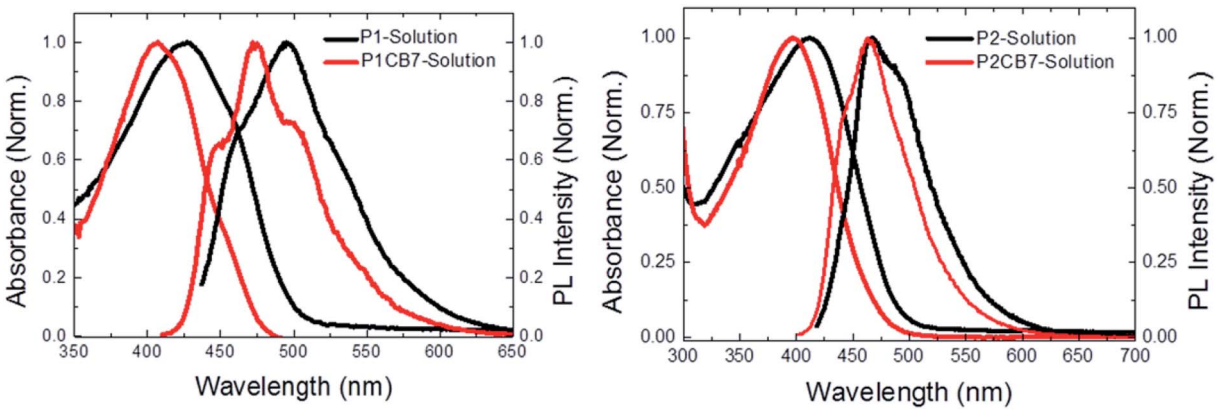

Fig. 4 UV-vis absorption and emission spectra of **P1**, **P2**, **P1CB7** and **P2CB7** in aqueous media.

higher temperatures. Thus, this clearly confirms the effect of CB on the thermal stability of polymers.

Photophysical properties

Blue shift was observed in the absorption and fluorescence maxima of **P1CB7** and **P2CB7** compared to **P1** and **P2**, respectively (Fig. 4) in aqueous media. This spectral shift was also observed in the solid state fluorescence spectra (Fig. 5). In both **P1CB7** and **P2CB7**, a great enhancement in both quantum yield efficiency and molar absorptivity was observed relative to **P1** and **P2**, respectively. The quantum yield efficiency and peak molar absorptivity of **P1CB7** in water was found to be 0.46 and 86 294 M^{-1} cm^{-1} compared to 0.11 and 26 563 M^{-1} cm^{-1} for **P1** (Table 2). Similarly the quantum yield efficiency and peak molar absorptivity of **P2CB7** in water was found to be 0.55 and 42 611 M^{-1} cm^{-1} compared to 0.35 and 28 376 M^{-1} cm^{-1} for **P2**. This enhancement could be attributed to the reduction of π–π interaction between the polymer chains. Moreover, while the solubility of the polymers in water is increased, the aggregate formation is decreased upon rotaxanation. The enhancement of quantum yield and molar absorptivity of **P2CB7** is less compared to **P1CB7** because of the lower threading efficiency in **P2CB7**.

We checked the fluorescence kinetics of the polymers through time resolved fluorescence spectroscopy. Fluorescence lifetime of **P1** and **P2** are 0.86 and 1.145 ns in solution state. When these are drop casted on quartz substrates, the fluorescence lifetimes decrease down to 0.036 and 0.161 ns for **P1** and **P2**, respectively. On the other hand, polyrotaxanes **P1CB7** and **P2CB7** show much longer fluorescence lifetime in their solid films (0.559 and 0.681 ns, respectively) as compared to their solutions (1.112 and 1.385 ns, respectively). The slow-down of the fluorescence decay in **P1CB7** and **P2CB7** as compared to their pristine versions (*i.e.*, **P1** and **P2**) indicates that the quenching of the threaded polymers is suppressed at the solid-state by blocking the formation of inter-chain quenching/trapping sites. Thus, this makes CB7-incorporated polymers appealing for potential applications including organic light emitting diodes (OLEDs). From Fig. 4–6 and Table 2, **P1CB7** showed increased of the fluorescence lifetime in both aqueous media and solid state compared to **P1**. Albeit the difference in life time of **P2CB7** and **P2** is not as large as the difference observed in the case of between **P1CB7** and **P1**. This can be explained by the previous argument of the low threading efficiency of **P2CB7**.

In order to further confirm that spectral changes mentioned above are because of the encapsulation of conjugated backbone

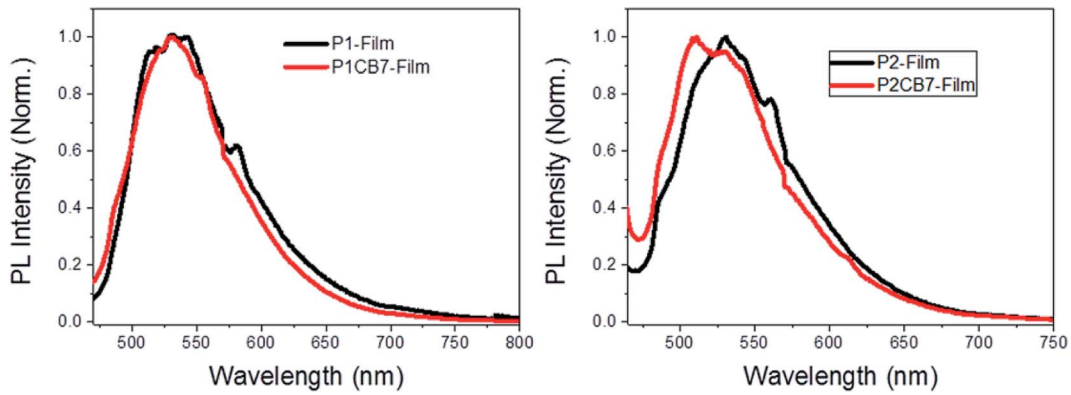

Fig. 5 Photoluminescence spectra of **P1**, **P2**, **P1CB7** and **P2CB7** in solid state.

Published on 11 October 2016. Downloaded by Bilkent University on 12/23/2018 11:24:34 AM.

Table 2 Photophysical properties of P1, P2, P1CB7 and P2CB7

	$\lambda_{max,solution}$[a] (nm)		$\lambda_{max,film}$[b] (nm)					
	UV	PL	PL	Φ_{PL}[c]	ε[d] (cm M)$^{-1}$	μ[e] (cm M)$^{-1}$	$\tau_{solution}$[f] (ns)	τ_{film}[g] (ns)
P1	427	501	541	0.11	26 563	2921	0.860	0.036
P1CB7	407	474	532	0.46	86 294	39 696	1.112	0.559
P2	413	465	528	0.35	28 376	9932	1.145	0.161
P2CB7	400	463	510	0.55	42 611	23 436	1.385	0.681

[a] In aqueous media. [b] On quartz. [c] Fluorescent quantum yields (Φ_{PL}) were measured relative to quinine sulfate 0.1 M H_2SO_4 ($\Phi_{PL} = 0.55$). [d] Molar absorptivity (per repeat unit). [e] Brightness (μ) = $\Phi_{PL} \times \varepsilon$. [f] Life time ($\tau$) in aqueous media. [g] Life time (τ) on quartz.

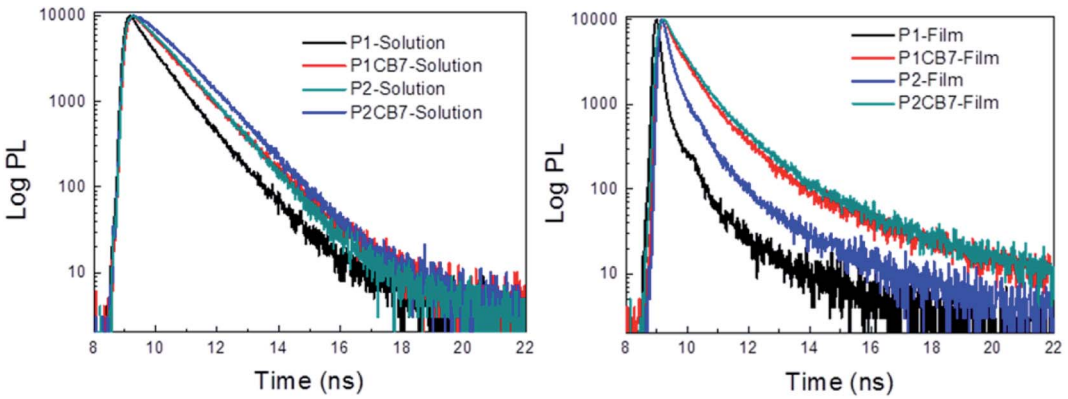

Fig. 6 Biexponentially fitted fluorescence lifetime decay curves of P1, P2, P1CB7 and P2CB7 in aqueous media and in solid state.

rather than complexation of CB7 with pendant or ammonium groups, optical properties of the aqueous solutions of physical mixtures of polymers **P1** and **P2** with CB7 at certain ratios (1 : 1, one equivalent per repeating unit of polymer/one equivalent CB7) were investigated by UV-vis absorption, steady-state and time-resolved fluorescent spectroscopies (see spectra in Fig. S15–S17, ESI†).

No spectral changes or shifts were observed in the absorption and emission wavelengths as well as in their fluorescent quantum yields of the samples of the physical mixtures in aqueous media with respect to polymers **P1** and **P2** (Fig. S15 and S16, ESI†).

However, the lifetimes of **P1** (0.860 ns) and **P2** (1.145 ns) decreased to 0.481 ns and 0.569 ns when they are physically mixed with CB7 (Fig. S17, ESI†); this is in marked contrast to the long lifetimes of polyrotaxanes which are 1.112 ns and 1.385 for **P1CB7** and **P2CB7**, respectively. These findings also confirm that the part of the conjugated backbone is encapsulated by CB7.

Electroluminescence properties

Enhanced mechanical and photophysical properties in the **P1CB7** and **P2CB7** polymers suggest that their electroluminescence performance in OLEDs could surpass those of the pristine polymers **P1** and **P2**. To test this hypothesis, we produced proof-of-concept solution-processed OLEDs having in the structure of ITO/PEDOT:PSS/poly-TPD/polymer/ZnO NPs/Al, where PEDOT:PSS/poly-TPD acts as hole injection-transport and electron blocking layers, and ZnO nanoparticles acts as electron injection and hole-blocking layer. The OLEDs are fabricated as described in the Experimental section. Fig. 7a shows the electroluminescence spectra of the OLED with **P1** polymer, which exhibited spectrally broad emission arising from both **P1** and poly-TPD hole-transport layer (peak at ~425 nm). This suggests that exciton formation is not complete in the OLED with **P1** emissive polymer layer. This could be either due to impeded hole injection into the **P1** or significant leakage of electrons into the poly-TPD layer through **P1**. In polyfluorene-based OLEDs, hole injection has been well-known to be quite limited due to low-lying HOMO levels in these polymers. Therefore, exciton formation is not efficient in the emissive polymer layer when using **P1**. In the case of OLED with **P1CB7** active emissive layer, the electroluminescence spectrum shows dominant **P1CB7** emission (see Fig. 7b). This strongly suggests that exciton formation is efficient in the **P1CB7** layer. This could be due to modification of the HOMO level in the **P1CB7** polymer. Moreover, better solid-state packing of the **P1CB7** polymer, which has shown significantly higher PL quantum yields as compared to its pristine counterpart, could also allow for the enhanced carrier injection and exciton formation in the active layer. Another observation is the lower turn-on voltages of the **P1CB7** OLEDs (<6 V) as compared to the one with **P1** (~9 V). This also highlights that overall charge injection is more favorable when using **P1CB7**. These observations make a point that introducing

 This journal is © The Royal Society of Chemistry 2016

Published on 11 October 2016. Downloaded by Bilkent University on 12/23/2018 11:24:34 AM.

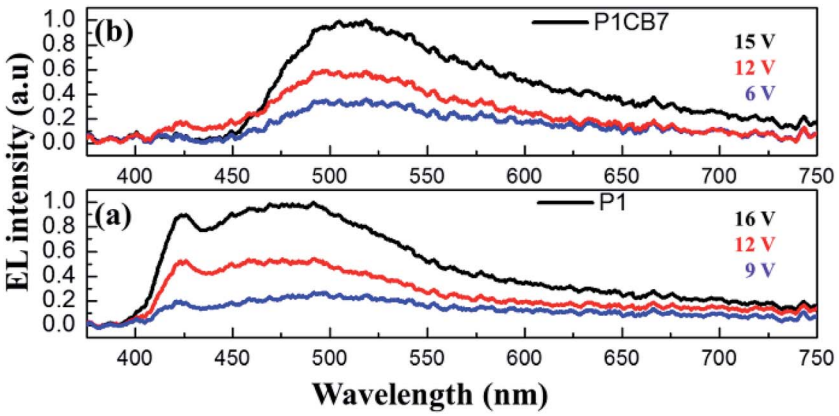

Fig. 7 The normalized electroluminescence spectra of the OLEDs that employ (a) **P1**, (b) **P1CB7** at different driving voltages.

CB7 group into the fluorene–thiophene based conjugated polyelectrolytes improves their electroluminescence performance as well.

Conclusions

Here, we have shown that the optical and thermal properties of fluorene–thiophene based conjugated polyelectrolytes could be altered by threading with CB7. Threading efficiency in **P1CB7** containing hexyl pendant was estimated to be as high as 50% but in the case of **P2** with propyl pendant was only around 15%. We attributed the threading efficiency differences to the steric effects caused by side chains of fluorene monomers in which propyl side chain serves as a rigid bulky group preventing the close proximity of monomers to react in the Suzuki coupling, whereas the hexyl side chain flex itself allowing the coupling to take place. The degree of threading manifest itself in the optical and thermal properties of the polymers. Fluorescent quantum yield of **P1** was measured as 0.11 but it increased about 5 folds (0.46) upon threading with CB7 (in **P1CB7**) whereas the fluorescent quantum yield of **P2** increased only 1.3 fold (from 0.35 to 0.55) in **P2CB7**. Moreover, threaded conjugated polyelectrolytes exhibited longer fluorescent lifetimes in the solution and the solid state as well as high thermal stabilities. Finally, we show that OLEDs employing CB7 containing fluorene–thiophene conjugated polymers exhibit considerably higher electroluminescence colour purity and lower turn-on voltages as compared to that of the pristine polymers thanks to the improved nanoscale morphology and photophysical properties in the CB7 threaded polymers.

Experimental section

All experimental details regarding the synthesis and characterization of monomers, polymers and polyrotaxanes were provided in the ESI† section.

Acknowledgements

We acknowledge TUBITAK-TBAG 112T058 and COST Action CM1005 (Supramolecular Chemistry in Water). We thank Dr Talha Erdem for his help in the measurement of some of the time resolved fluorescence spectra, reading our manuscript and providing insightful comments.

References

1 A. Facchetti, *Chem. Mater.*, 2011, **23**, 733–758.
2 A. C. Grimsdale, K. L. Chan, R. E. Martin, P. G. Jokisz and A. B. Holmes, *Chem. Rev.*, 2009, **109**, 897–1091.
3 D. T. McQuade, A. E. Pullen and T. M. Swager, *Chem. Rev.*, 2000, **100**, 2537–2574.
4 E. Smela, *Adv. Mater.*, 2003, **15**, 481–494.
5 G. M. Farinola and R. Ragni, *Chem. Soc. Rev.*, 2011, **40**, 3467–3482.
6 H. Wu, L. Ying, W. Yang and Y. Cao, *Chem. Soc. Rev.*, 2009, **38**, 3391–3400.
7 C. Zhu, L. Liu, Q. Yang, F. Lv and S. Wang, *Chem. Rev.*, 2012, **112**, 4687–4735.
8 F. Huang, H. Wu and Y. Cao, *Chem. Soc. Rev.*, 2010, **39**, 2500–2521.
9 S. Rochat and T. M. Swager, *J. Am. Chem. Soc.*, 2013, **135**, 17703–17706.
10 S. H. Lee, S. Komurlu, X. Zhao, H. Jiang, G. Moriena, V. D. Kleiman and K. S. Schanze, *Macromolecules*, 2011, **44**, 4742–4751.
11 A. Duarte, K.-Y. Pu, B. Liu and G. C. Bazan, *Chem. Mater.*, 2011, **23**, 501–515.
12 P. B. Balanda, M. B. Ramey and J. R. Reynolds, *Macromolecules*, 1999, **32**, 3970–3978.
13 K. Liu, Y. Yao, Y. Kang, Y. Liu, Y. Han, Y. Wang, Z. Li and X. Zhang, *Sci. Rep.*, 2013, **3**, 2372.
14 T. Heek, C. Fasting, C. Rest, X. Zhang, F. Wurthner and R. Haag, *Chem. Commun.*, 2010, **46**, 1884–1886.
15 S. Kirmayer, E. Dovgolevsky, M. Kalina, E. Lakin, S. Cadars, J. D. Epping, A. Fernández-Arteaga, C. Rodríguez-Abreu, B. F. Chmelka and G. L. Frey, *Chem. Mater.*, 2008, **20**, 3745–3756.
16 B. Zhu, Y. Han, M. Sun and Z. Bo, *Macromolecules*, 2007, **40**, 4494–4500.
17 G. Wenz, B.-H. Han and A. Müller, *Chem. Rev.*, 2006, **106**, 782–817.

Published on 11 October 2016. Downloaded by Bilkent University on 12/23/2018 11:24:34 AM.

18 M. J. Frampton and H. L. Anderson, *Angew. Chem., Int. Ed.*, 2007, **46**, 1028–1064.
19 J. Terao, *Polym. Chem.*, 2011, **2**, 2444–2452.
20 J. J. Michels, M. J. O'Connell, P. N. Taylor, J. S. Wilson, F. Cacialli and H. L. Anderson, *Chem.–Eur. J.*, 2003, **9**, 6167–6176.
21 F. Cacialli, J. S. Wilson, J. J. Michels, C. Daniel, C. S. Silva, R. H. Friend, N. Severin, P. Samorì, J. P. Rabe, M. J. O'Connell, P. N. Taylor and H. L. Anderson, *Nat. Mater.*, 2002, **1**, 160–164.
22 Y. Ling and A. E. Kaifer, *Chem. Mater.*, 2006, **18**, 5944–5949.
23 R. Eelkema, K. Maeda, B. Odell and H. L. Anderson, *J. Am. Chem. Soc.*, 2007, **129**, 12384–12385.
24 N. Willis-Fox, C. Belger, J. F. Fennell Jr, R. C. Evans and T. M. Swager, *Chem. Mater.*, 2016, **28**, 2685–2691.
25 D. Tuncel, M. Artar and S. B. Hanay, *J. Polym. Sci., Part A: Polym. Chem.*, 2010, **48**, 4894–4899.
26 K. I. Assafa and W. M. Nau, *Chem. Soc. Rev.*, 2015, **44**, 394–418.
27 S. J. Barrow, S. Kasera, M. J. Rowland, J. del Barrio and O. A. Scherman, *Chem. Rev.*, 2015, **115**, 12320–12406.
28 S. Gürbüz, M. Idris and D. Tuncel, *Org. Biomol. Chem.*, 2015, **13**, 330–347.
29 E. Masson, X. Ling, R. Joseph, L. Kyeremeh-Mensah and X. Lu, *RSC Adv.*, 2012, **2**, 1213–1247.
30 K. Kim, N. Selvapalam, Y. H. Ko, K. M. Park, D. Kim and J. Kim, *Chem. Soc. Rev.*, 2007, **36**, 267–279.
31 D. Tuncel, O. Unal and M. Artar, *Isr. J. Chem.*, 2011, **51**, 525–532.
32 J. Pennakalathil, E. Jahja, E. S. Özdemir, Ö. Konu and D. Tuncel, *Biomacromolecules*, 2014, **15**, 3366–3374.
33 R. N. Dsouza, U. Pischel and W. M. Nau, *Chem. Rev.*, 2011, **111**, 7941–7980.
34 A. Hennig, H. Bakirci and W. M. Nau, *Nat. Methods*, 2007, **4**, 629–632; O. Huyal, T. Ozel, U. Koldemir, S. Nizamoglu, D. Tuncel and H. V. Demir, *Opt. Express*, 2008, **16**, 1115–1124.
35 O. Huyal, U. Koldemir, T. Ozel, H. V. Demir and D. Tuncel, *J. Mater. Chem.*, 2008, **18**, 3568–3574.
36 V. İbrahimova, S. Ekiz, O. Gezici and D. Tuncel, *Polym. Chem.*, 2011, 2818–2824.
37 B. Guzelturk, P. L. Hernandez-Martinez, V. K. Sharma, Y. Coskun, V. Ibrahimova, D. Tuncel, A. O. Govorov, X. W. Sun, Q. Xiong and H. V. Demir, *Nanoscale*, 2014, **6**, 11387–11394.

This journal is © The Royal Society of Chemistry 2016